Leading Λ production in future electron-proton colliders

F. Carvalho and K. P. Khemchandani
Departamento de Ciências Exatas e da Terra, Universidade Federal de São Paulo, Campus Diadema, Rua Prof. Artur Riedel, 275, Jd. Eldorado, 09972-270, Diadema, SP, Brazil

V. P. Gonçalves
Institut für Theoretische Physik, Westfälische Wilhelms-Universität Münster, Wilhelm-Klemm-Straße 9, D-48149 Münster, Germany and Institute of Physics and Mathematics, Federal University of Pelotas, Postal Code 354, 96010-900, Pelotas, RS, Brazil

F. S. Navarra, D. Spiering, and A. Martínez Torres
Instituto de Física, Universidade de São Paulo, C.P. 66318, 05315-970 São Paulo, SP, Brazil

(Received 25 June 2023; accepted 6 October 2023; published 27 November 2023)

Leading Λ (LL) production in ep collisions at high energies is investigated using the color dipole formalism and taking into account the nonlinear QCD effects. In particular, the impact of the absorptive effects on the LL spectra are estimated considering the kinematical range that will be probed by the Electron Ion Collider and by the Large Hadron electron Collider. Our results indicate that the LL spectrum is strongly suppressed at small photon virtualities. These results suggest that absorptive effects are not negligible and should be taken into account in order to extract the kaon structure function from data on leading Λ production.

DOI: 10.1103/PhysRevD.108.094034

I. INTRODUCTION

The experimental data from HERA, RHIC, and LHC have largely improved our understanding of the proton structure during the last decades (for a review see, e.g., Ref. [1]). In particular, the data from the HERA ep collider have demonstrated that for high energies and small values of the Bjorken-x variable, the proton is composed by a large number of gluons, which motivated a large number of theoretical studies about the QCD dynamics at high partonic densities [2]. The observation of nonlinear effects in the QCD dynamics is one of the main motivations for the construction of the future electron-hadron colliders at BNL (EIC) [3] and at CERN (LHeC) [4]. In addition, these colliders are expected to probe the 3D structure of the proton encoded in the quantum phase space Wigner distributions, which include information on both generalized parton distributions (GPDs) and transverse momentum parton distributions (TMDs). As a consequence, a deeper understanding of the proton structure is expected to be reached in the forthcoming years.

A natural question is if a similar improvement of our understanding of the pion and kaon structure can also be reached in the near future (see e.g. Ref. [5]). Such a challenge has motivated a large number of studies based on the meson cloud model of the proton [6], which have proposed different ways of constraining the meson structure in ep and pp colliders [7–17]. The basic idea is that the proton may be decomposed in a series of Fock states, containing states such as $|\pi^+ n\rangle$ and $|K^+\Lambda\rangle$, and that these states can be probed in the interaction with a given projectile. Therefore, the virtual photon present in ep collisions can be used to probe the meson structure, with the process being characterized by a leading baryon that acts as a spectator carrying a large fraction of the incoming proton momentum and having a very large rapidity. In the last decades, this formalism has been applied to leading neutron production at HERA [7–17], which have improved our understanding of the pion structure. In particular, in Refs. [14,15], the color dipole (CD) formalism, which successfully describes the ep HERA data and allows us to take into account the nonlinear QCD dynamical effects, has been extended to leading baryon production in inclusive and exclusive processes. As demonstrated in Refs. [14,15], the CD formalism is able to describe the current leading

Published by the American Physical Society under the terms of the Creative Commons Attribution 4.0 International license. Further distribution of this work must maintain attribution to the author(s) and the published article's title, journal citation, and DOI. Funded by SCOAP³.

neutron data and important improvements are expected in the future ep colliders. One of the goals of this paper is to extend the CD formalism to leading Λ production and present predictions for the EIC and LHeC.

Another goal of this work is to estimate, for the first time, the impact of the absorptive effects on leading Λ production in ep collisions. The absorptive effects (denoted S^2_{eik} hereafter) are associated with soft rescatterings between the produced and spectator particles, which can break the validity of the factorization hypothesis. This hypothesis allows us to factorize the cross section in terms of the $p \to MB$ splitting and photon-meson interaction. As a consequence, a precise determination of S^2_{eik} is fundamental in order to access the meson structure. The studies performed in Refs. [18–21] indicated that these effects strongly affect leading neutron production in pp collisions. In contrast, the absorptive corrections are predicted to be smaller in ep collisions and their effects become weaker at larger photon virtualities [18,22–24]. In particular, in Ref. [24], one has applied the CD formalism to estimate S^2_{eik} in the leading neutron production at ep colliders. In this paper, we will extend the analysis performed in Ref. [24] to the leading Λ production and will estimate its impact for different center-of-mass energies and different photon virtualities. Moreover, a comparison with the results derived for leading neutron production will also be presented. The results presented in this paper are a necessary step to allow us, in the future, to obtain a realistic description of the kaon structure.

This paper is organized as follows. In the next section we will address leading Λ production in ep collisions and present its description in the color dipole formalism. The main ingredients needed for the calculation of the spectrum will be briefly reviewed. Moreover, we will discuss the absorptive effects and present our assumptions for the dipole-kaon cross section. Our results will be presented in Sec. III considering different values of the center-of-mass energy and several photon virtualities. A comparison with the results derived for leading neutron production will be presented. Finally, in Sec. IV we will summarize our main results and conclusions.

II. LEADING Λ SPECTRUM IN THE COLOR DIPOLE FORMALISM

The kaon structure can be probed in electron-proton collisions through the Sullivan process [6], where the electron scatters off the meson cloud of the proton target. The associated processes can be separated by tagging a forward Λ in the final state, which carries a large fraction of the proton energy. Theoretically, this leading Λ production is usually described assuming that the splitting $p \to \Lambda K$ and the photon-kaon interaction can be factorized, as represented in Fig. 1, where $f_{K/p}$ represents the kaon flux. Assuming the validity of the factorization hypothesis and the universality of the fragmentation process, which allows us to constrain $f_{K/p}$ using the data of leading Λ production in pp collisions, we can obtain $\sigma_{\gamma^* K}$ and, consequently, determine the x and Q^2 dependence of the kaon structure function. Following Refs. [14,15] we propose to treat leading Λ production in ep processes with the color dipole formalism. In this model, the virtual photon-kaon cross section can be factorized in terms of the photon wave function (which describes the photon splitting in a $q\bar{q}$ pair) and the dipole-kaon cross section σ_{dK} (see Fig. 1). As shown in Refs. [14,15], the HERA data on leading neutron production are quite well described by this approach assuming that absorptive corrections can be factorized and represented by a multiplicative constant factor, denoted by K_{abs} in Ref. [14].

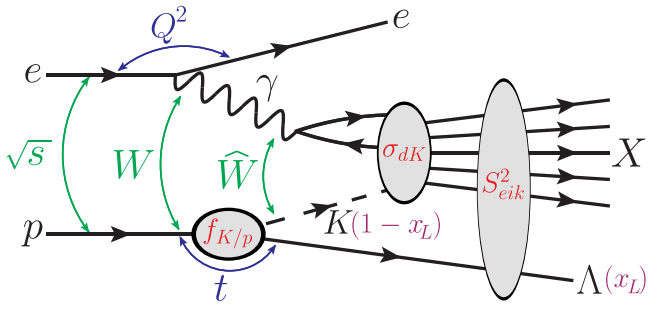

FIG. 1. Leading Λ production in $ep \to e\Lambda X$ interactions at high energies in the color dipole model.

Let us first recall the expressions proposed in Ref. [14] to treat leading neutron production in ep collisions, adapting them to leading Λ production. Disregarding initially the absorptive effects ($S^2_{eik} = 1$), this process can be seen as a set of three factorizable subprocesses: (i) the photon emitted by the electron fluctuates into a quark-antiquark pair (the color dipole), (ii) the color dipole interacts with the kaon, and (iii) the leading Λ is formed. In the color dipole formalism, the differential cross section reads:

$$\frac{d^2\sigma(W,Q^2,x_L)}{dx_L} = \int dt f_{K/p}(x_L,t) \times \sigma_{\gamma^* K}(\hat{W}^2,Q^2), \tag{1}$$

$$= \int dt f_{K/p}(x_L,t) \times \int_0^1 dz \int d^2\boldsymbol{r} \sum_{L,T} |\Psi_{T,L}(z,\boldsymbol{r},Q^2)|^2 \sigma_{dK}(x_K,\boldsymbol{r}), \tag{2}$$

where Q^2 is the virtuality of the exchanged photon, x_L is the proton momentum fraction carried by the Λ, and t is the square of the four-momentum of the exchanged kaon. Moreover, $\hat{W}$ is the center-of-mass energy of the virtual photon-kaon system, which can be written as $\hat{W}^2 = (1-x_L)W^2$, where W is the center-of-mass energy of the virtual photon-proton system. In terms of the measured quantities x_L and transverse momentum p_T of the Λ, the kaon virtuality is

$$t \simeq -\frac{p_T^2}{x_L} - \frac{(1-x_L)(m_\Lambda^2 - m_p^2 x_L)}{x_L}. \tag{3}$$

In Eq. (2), the virtual photon-kaon cross section was expressed in terms of the transverse and longitudinal photon wave functions Ψ_i, which describe the photon splitting into a $q\bar{q}$ pair of size $r \equiv |\boldsymbol{r}|$, and the dipole-kaon cross section σ_{dK}, which is determined by the QCD dynamics at high energies [2]. The variable z represents the longitudinal photon momentum fraction carried by the quark, the variable r defines the relative transverse separation of the pair (dipole), and the scaling variable x_K is defined by $x_K = x/(1-x_L)$, where x is the Bjorken variable. As in Ref. [14], we will assume that this quantity can be related to the dipole-proton cross section through $\sigma_{dK} = R_q \cdot \sigma_{dp}$, with $R_q = 2/3$ as in the additive quark model. Moreover, σ_{dp} will be described by the color glass condensate (CGC) formalism, as given in the phenomenological model proposed in Ref. [25]. As a consequence, we will have that

$$\begin{aligned}\sigma_{dK}(x,\boldsymbol{r}) &= \frac{2}{3}\cdot\sigma_{dp}(x,\boldsymbol{r}) \\ &= \frac{2}{3}\cdot 2\pi R_p^2 \times \begin{cases} \mathcal{N}_0\left(\frac{rQ_s}{2}\right)^{2\left(\gamma_s + \frac{\ln(2/rQ_s)}{\kappa\lambda\gamma}\right)}, & \text{for } rQ_s(x) \le 2, \\ 1 - \mathrm{e}^{-a\ln^2(brQ_s)}, & \text{for } rQ_s(x) > 2, \end{cases}\end{aligned} \tag{4}$$

where a and b are determined by continuity conditions at $rQ_s(x) = 2$. The parameters $\gamma_s = 0.7376$, $\kappa = 9.9$, $\mathcal{N}_0 = 0.7$, and $R_p = 3.344\ \mathrm{GeV}^{-1}$ have been adjusted using the HERA data in Ref. [26], with the saturation scale Q_s given by

$$Q_s^2(x) = Q_0^2\left(\frac{x_0}{x}\right)^\lambda \tag{5}$$

with $x_0 = 1.632 \times 10^{-5}$, $\lambda = 0.2197$, $Q_0^2 = 1.0\ \mathrm{GeV}^2$. The first line of Eq. (4) describes the linear regime whereas the second one includes saturation effects. This model is of course not the only one and there are several others in the literature. In order to have an idea of how our results depend on the choice of the dipole cross section, we will also consider the model presented in Ref. [27].

The flux factor $f_{K/p}$ gives the probability of the splitting of a proton into a K-Λ system and can be expressed as follows (see e.g. Ref. [18])

$$f_{K/p}(x_L,t) = \frac{1}{2}\pi\sum_{\lambda\lambda'}|\phi_{\Lambda K}^{\lambda\lambda'}(x_L,\mathbf{p}_T)|^2 \tag{6}$$

where $\phi_{\Lambda K}^{\lambda\lambda'}(x_L,\mathbf{p}_T)$ is the probability amplitude to find, inside a proton with spin up, a Λ with longitudinal momentum fraction x_L, transverse momentum $\mathbf{p}_T$ and helicity λ and a kaon, with longitudinal momentum fraction $1-x_L$, transverse momentum $-\mathbf{p}_T$ and helicity λ'. In the light-cone approach, the amplitudes $\phi_{\Lambda K}$ of a proton with spin $+1/2$, read

$$\begin{aligned}\phi_{\Lambda K}^{1/2,0}(x_L,\mathbf{p}_T) &= \frac{g_0}{4\pi}\sqrt{\frac{3}{2\pi}}\frac{1}{\sqrt{x_L^2(1-x_L)}}\frac{(x_L m_N - m_\Lambda)}{M_{\Lambda K}^2 - m_N^2}, \\ \phi_{\Lambda K}^{-1/2,0}(x_L,\mathbf{p}_T) &= \frac{g_0}{4\pi}\sqrt{\frac{3}{2\pi}}\frac{1}{\sqrt{x_L^2(1-x_L)}}\frac{|\mathbf{p}_T|e^{-i\varphi}}{M_{\Lambda K}^2 - m_N^2},\end{aligned} \tag{7}$$

where $M_{\Lambda K}^2$ is the invariant mass of the K-Λ system, given by

$$M_{\Lambda K}^2 = \frac{m_\Lambda^2 + p_T^2}{x_L} + \frac{m_K^2 + p_T^2}{1-x_L},$$

with m_Λ and m_K being the Λ and the kaon masses, g_0 is the $NK\Lambda$ coupling constant [28], and φ is the azimuthal angle in the transverse plane. Because of the extended nature of the hadrons involved, the interaction amplitudes in the above equations have to be modified by including a phenomenological $NK\Lambda$ form factor, $G(x_L,p_T)$. It is important to stress here that while the vertex is derived from an effective meson-nucleon Lagrangian, the form factor is introduced *ad hoc*. In our analysis we will choose the covariant form factor, corrected by the Regge factor, given by

$$G(x_L,p_T) = \exp[R_c^2(t-m_K^2)](1-x_L)^{-\alpha_0 t} \tag{8}$$

where $\alpha_0 = 1\ \mathrm{GeV}^{-2}$ and $R_c^2 = 0.3\ \mathrm{GeV}^{-2}$ were constrained using the HERA data (for details see Ref. [14]). The amplitude $\phi_{\Lambda K}^{\lambda\lambda'}(x_L,\mathbf{p}_T)$ changes to $\phi_{\Lambda K}^{\lambda\lambda'}(x_L,\mathbf{p}_T)\times G(x_L,p_T)$ and then the kaon flux becomes

$$f_{K/p}(x_L,t) = \frac{1}{2}\pi\sum_{\lambda\lambda'}|\phi_{\Lambda K}^{\lambda\lambda'}(x_L,\mathbf{p}_T)|^2|G(x_L,p_T)|^2, \tag{9}$$

where $1/2$ is the isospin factor and the azimuthal angle in the transverse plane has been integrated out.

In order to derive more realistic predictions for the leading Λ spectrum it is crucial to improve the description of S^2_{eik}. This was done in Ref. [24] for leading neutron production, where we revisited and updated the approach proposed in Ref. [18] to study absorptive effects. In order to include the absorptive effects in our predictions for the leading Λ spectrum $d\sigma/dx_L$, we will follow the approach proposed in Ref. [18], where these effects were estimated using the high-energy Glauber approximation [29] to treat the multiple scatterings between the dipole and the K-Λ system. As demonstrated in Ref. [18], such approach can be easily implemented in the impact parameter space, implying that the spectrum can be expressed as follows:

$$\frac{d\sigma(W,Q^2,x_L)}{dx_L} = \int d^2\boldsymbol{b}_{\rm rel}\rho_{\Lambda K}(x_L,\boldsymbol{b}_{\rm rel}) \int dz d^2\boldsymbol{r} \sum_{L,T} |\Psi_{T,L}(z,\boldsymbol{r},Q^2)|^2 \sigma_{dK}(x_K,\boldsymbol{r}) S^2_{eik}(\boldsymbol{r},b_{\rm rel}), \tag{10}$$

where $\rho_{\Lambda K}(x_L,\boldsymbol{b}_{\rm rel})$ is the probability density of finding a Λ and a kaon with momenta x_L and $1-x_L$, respectively, and with a relative transverse separation $b_{\rm rel}$, which is given by

$$\rho_{\Lambda K}(x_L,\boldsymbol{b}_{\rm rel}) = \sum_i |\psi^i_{\Lambda K}(x_L,\boldsymbol{b}_{\rm rel})|^2 \tag{11}$$

with

$$\psi^i_{\Lambda K}(x_L,\boldsymbol{b}_{\rm rel}) = \frac{1}{2\pi}\int d^2\mathbf{p}_T e^{i\boldsymbol{b}_{\rm rel}\cdot\mathbf{p}_T}\phi^i_{\Lambda K}(x_L,\mathbf{p}_T), \tag{12}$$

and $\phi^i_{\Lambda K} = \sqrt{2/3}\phi^{\lambda\lambda'}_{\Lambda K} G(x_L,p_T)$. Moreover, the survival factor S^2_{eik} associated to the absorptive effects is expressed in terms of the dipole Λ ($\sigma_{d\Lambda}$) cross section as follows:

$$S^2_{eik}(\boldsymbol{r},b_{\rm rel}) = \left\{1 - \Lambda^2_{\rm eff}\frac{\sigma_{d\Lambda}(x_\Lambda,\boldsymbol{r})}{2\pi}\exp\left[-\frac{\Lambda^2_{\rm eff}\boldsymbol{b}^2_{\rm rel}}{2}\right]\right\}, \tag{13}$$

where $x_\Lambda = x/x_L$ and $\Lambda^2_{\rm eff}$ is an effective parameter that was found to be equal to 0.1 GeV^2 in Ref. [18].

As can be seen from the above expression, the absorptive corrections depend crucially on the dipole-Lambda cross section, $\sigma_{d\Lambda}$. In our previous work [24] on the leading neutron spectrum, we assumed that σ_{dn} was equal to the dipole-proton cross section, σ_{dp}, which is strongly constrained by HERA data. While this was a good approximation for σ_{dn}, this may be not so good for $\sigma_{d\Lambda}$. What is the effect of changing a light quark by a strange quark in the baryon which scatters against the dipole? We can try to answer this question comparing the data on pp and $\Sigma^- p$ cross sections measured at $\sqrt{s}\simeq 30$ GeV. This energy is relevant for the study of HERA data, where the dipole-baryon collisions happen at $\hat{W} = \sqrt{1-x_L}W$. Considering values of W in the range $100 < W < 200$ GeV and assuming that $x_L \simeq 0.7$ the dipole-baryon collision energies are typically 50–100 GeV. At these energies the data and the parametrizations performed in Ref. [30] yield $\sigma_{p\Sigma^-} \simeq 0.8\sigma_{pp}$. This suggests that, in a first approximation, $\sigma_{d\Lambda} \simeq 0.8\sigma_{dn}$. Going from HERA to the LHeC, $\hat{W}$ would be much higher (≃500 GeV) and according to [30] the differences between the cross sections would decrease. On the other hand, going from HERA to JLab we have $\hat{W} = 5$–10 GeV. In order to have an estimate of the dipole-baryon cross section at low energies, in the Appendix we have computed the $\pi - n$ and $\pi - \Lambda$ cross sections using a effective Lagrangian theory [31,32] and found that it predicts that strange baryons have smaller cross section than the light baryons. These findings are in agreement with old data [33] and also with other calculations [34], indicating that $\sigma_{p\Lambda} \simeq 0.8\sigma_{pp}$. Taken together, these results are a strong indication that $\sigma_{d\Lambda} = r_s\sigma_{dp}$, with $r_s \approx \text{const} \leq 1$. As we will demonstrate in the next section, when such an assumption is applied to our study, it has the interesting consequence that leading Λ's have a smaller production cross section but are less absorbed than leading neutrons.

III. RESULTS

In this section we will present the color dipole model predictions for leading Λ production in ep collisions at the EIC and LHeC.

Initially, in Fig. 2(a) we present the leading Λ spectrum at different energies. We focus on the dependence of the results on the choice of the dipole cross section. The solid lines show the results obtained with the IIM [25] dipole cross section. Dashed lines represent the results obtained with the GBW [27] dipole cross section. We can see that the predictions are similar, which is expected since the leading Lambda spectrum is computed at values of the variable x which are not so small. In this region of the phase space the dipole cross sections are strongly constrained by the existing data and, as a consequence, the predictions tend to agree with each other. However, for higher energies and much lower values of x, beyond those probed at the EIC and LHeC, different dipole cross sections are expected to lead to different results. Figure 2(b) shows the dependence of the spectrum on the parameter $\Lambda_{\rm eff}$ which appears in the survival factor S^2_{eik}. As demonstrated in Ref. [18], this parameter can be expressed, in a first approximation, in terms of the cross sections for the pion-pion and rho meson-neutron processes. Using the typical values for LHC

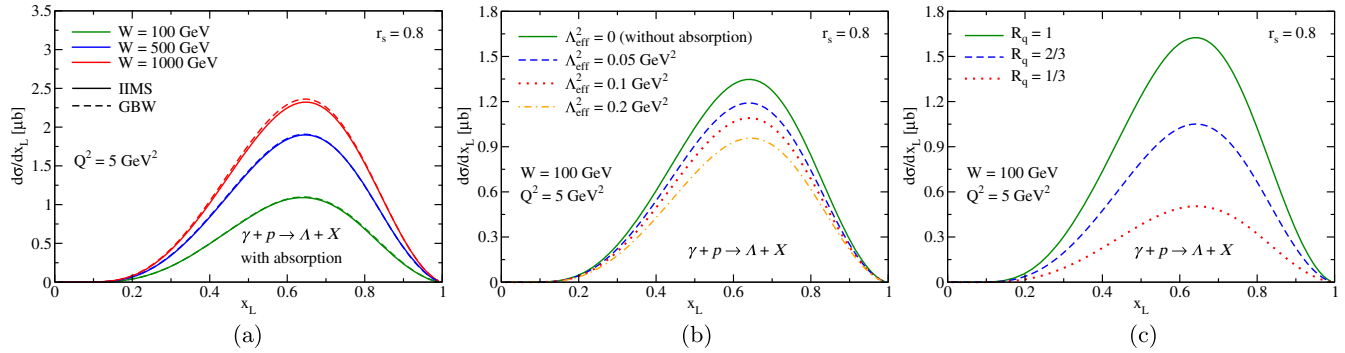

FIG. 2. (a) Leading Λ spectrum at different energies. Dependence of the results on the choice of the dipole cross section. The solid lines show the results obtained with the IIM dipole cross section, used throughout this work. Dashed lines represent the results obtained with the GBW dipole cross section. (b) Dependence of the spectrum on the parameter $\Lambda_{\rm eff}$ which appears in the survival factor S^2_{eik}. (c) Dependence of the spectrum on the parameter R_q. $R_q = 2/3$ is the prediction of the additive quark model, used throughout this work.

energies, we find that $\Lambda^2_{\rm eff} \approx 0.1$ GeV^2, which is the value used throughout this work. However, the results presented in Fig. 2(b) indicate that our predictions are modified by ≈20% if $\Lambda^2_{\rm eff}$ is modified by a factor 2. Figure 2(c) illustrates the dependence of the spectrum on the parameter R_q. In our analysis, we have assumed $R_q = 2/3$, motivated by the additive quark model. However, as this factor determines the normalization of the dipole-kaon cross section, our predictions for the spectrum are strongly dependent on this parameter. Currently, our main justification to assume $R_q = 2/3$ is associated to the fact that this assumption allow us to describe the HERA data on the leading neutron production.

In Fig. 3(a) we present our prediction for the spectrum in the HERA kinematical region, assuming that $Q^2 = 53$ GeV^2, $W = 100$ GeV, and $r_s = 0.8$. For comparison, we also present the results derived in Ref. [14] and the associated H1 data [35]. It is important to emphasize that our predictions are expected to be valid in the region $x_L \gtrsim 0.5$, since for smaller values of x_L, additional contributions are expected to play a significant role [19,21]. The cross section for leading Λ production is smaller than that for leading neutron production, with the peak occurring for $x_L \approx 0.6$. In Fig. 3(b) we analyze the dependence of our prediction on the value of r_s, which is the scale factor that determines the relation between the dipole-Lambda and dipole-proton cross sections. As it can be seen, larger values of r_s imply a reduction of the spectrum, which is expected since the impact of the absorptive effects are larger when $\sigma_{d\Lambda}$ increases [see Eq. (13)]. In Fig. 3(c) we present our predictions for the Λ spectra at different center-of-mass energies, $Q^2 = 5$ GeV^2 and $r_s = 0.8$. We find that the predictions are not strongly dependent on W, similarly to what was observed in leading neutron production in Ref. [14]. Such results demonstrate that the color dipole formalism predicts that the leading baryon spectrum leads to Feynman scaling, i.e. the energy independence of the x_L spectra.

As discussed in the previous section, in order to measure the $\gamma\pi$ and γK cross sections and extract, respectively, the pion and kaon structure functions, it is crucial to have control of the absorptive effects. In particular, we should know the dependence of these effects on Q^2, W, and x_L. We can estimate the impact of the absorptive effects through the calculation of the ratio between the cross sections with and without absorption, defined by

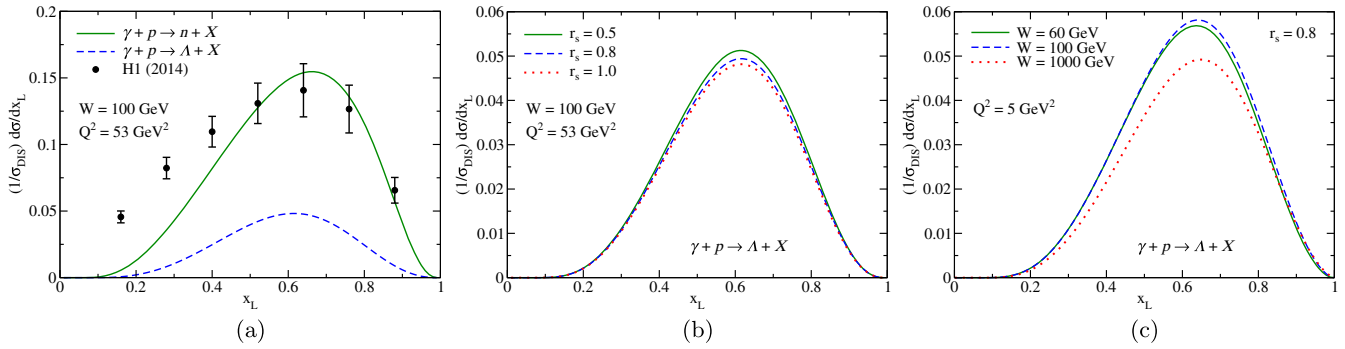

FIG. 3. (a) Predictions of the color dipole formalism for leading Λ production in the HERA kinematical range. For comparison, the results for leading neutron production and corresponding HERA data [35] are also presented. (b) Dependence on r_s of the leading Λ spectrum. (c) Dependence of the leading Λ spectrum on the photon-proton center-of-mass energy W for $Q^2 = 5$ GeV^2.

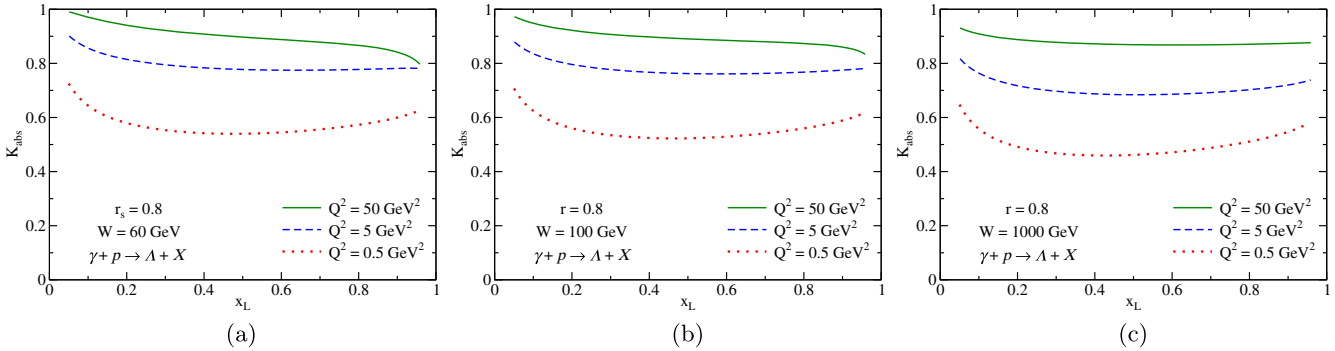

FIG. 4. Dependence of the absorptive effects on x_L in leading Λ production in ep collisions for different values of the photon virtuality. (a) $W = 60$ GeV, (b) $W = 100$ GeV, and (c) $W = 1000$ GeV.

$$K_{abs}(W, Q^2, x_L) = \frac{\frac{d\sigma}{dx_L}[S^2_{eik}]}{\frac{d\sigma}{dx_L}[S^2_{eik} = 1]}. \tag{14}$$

In the case of leading Λ production, our predictions for this ratio, obtained assuming $r_s = 0.8$, are presented in Fig. 4. Our results show that the impact increases for smaller values of Q^2 and it is almost insensitive to the energy W. For $Q^2 = 50$ GeV^2, we see that $K_{abs} \approx 0.9$ for $x_L \gtrsim 0.5$, with the predictions being similar for the three values of W. This weak absorption is expected in the color dipole formalism, since at large values of Q^2 the main contribution to the cross section comes from dipoles with a small pair separation. In this regime, known as color transparency, the impact of the rescatterings is small, which implies that the absorptive effects become negligible. Similar results were derived in Refs. [18,24]. On the other hand, for small virtualities ($Q^2 = 0.5$ GeV^2), we observe strong absorptive effects, which reduce the cross sections by a factor $\approx$0.5 for $x_L = 0.5$. This result is also expected, since for small Q^2 the cross section is dominated by large dipoles and, consequently, the contribution of the rescatterings cannot be disregarded. For larger values of x_L, absorptive effects cannot be modeled by a constant factor. Our conclusions agree with those derived in Ref. [21] using Regge theory. Finally, our results indicate that the contribution of the absorptive effects is not strongly energy dependent. This result suggests that the main conclusion of Ref. [14], that the spectra will satisfy Feynman scaling, is still valid when the absorptive effects are estimated using a more realistic model.

In Fig. 5 we present a comparison between the absorptive factors estimated for the leading neutron and leading Λ productions at the EIC energy ($W = 100$ GeV) considering different values of Q^2. Moreover, the leading Λ predictions are presented for three distinct values of r_s. As expected from the results discussed above, these predictions are strongly dependent on r_s, with $K^{\Lambda}_{abs} \geq K^{n}_{abs}$ for $r_s \lesssim 0.8$ and intermediated values of x_L, indicating that the Λ's are less absorbed in comparison to leading neutrons. This can be qualitatively understood as follows. The production cross section is given by Eq. (10). This equation is more detailed but (if we disregard for a moment the absorption factor S_{eik}) it has the same physical content of Eq. (2), which is more transparent. The leading baryon cross section depends on two factors: the splitting function $f_{p\to BM}$ and the photon-meson cross section $\sigma_{\gamma M}$. The function f comes from a Feynman diagram which depends on masses and couplings (see, for example, Ref. [6] for leading neutrons and Ref. [36] for leading Lambdas). It is

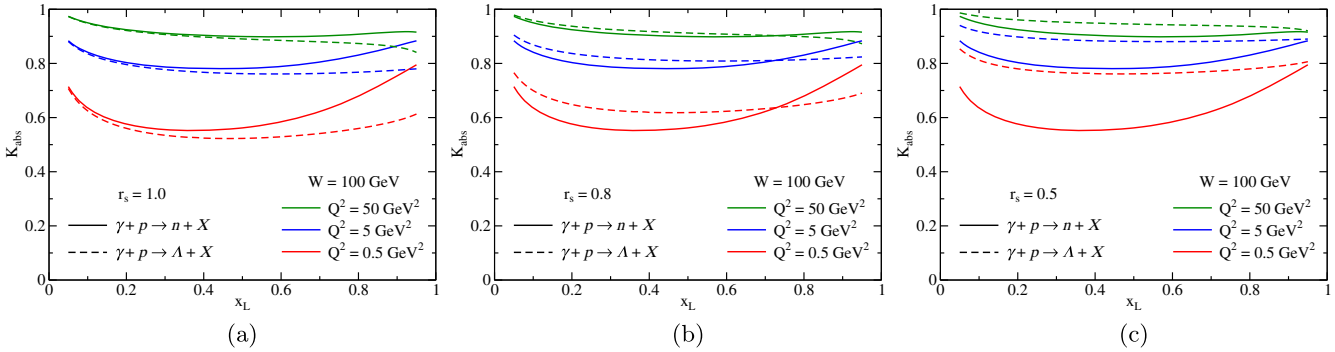

FIG. 5. Comparison of the absorptive effects in leading neutron and leading Λ production in ep collisions at the EIC energy ($W = 100$ GeV) for different photon virtualities Q^2 and different values of r_s: (a) $r_s = 1.0$, (b) $r_s = 0.8$, and (c) $r_s = 0.5$.

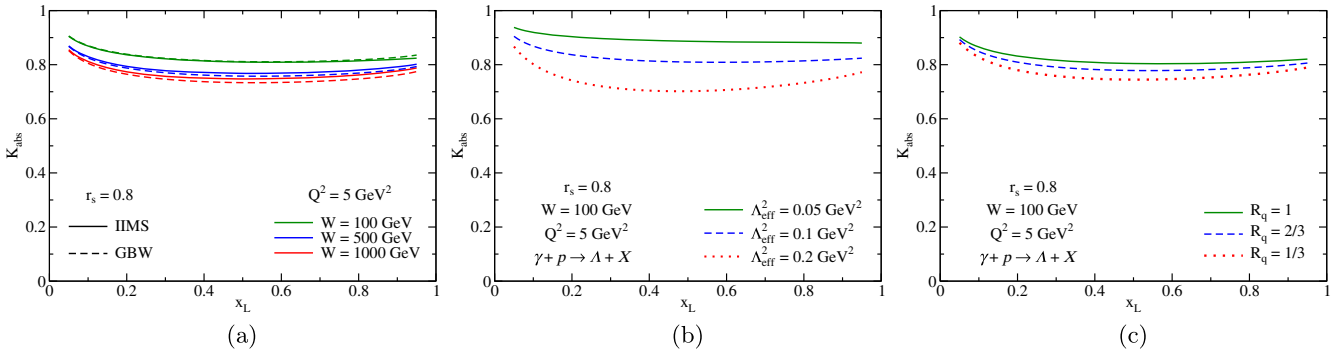

FIG. 6. Dependence of the ratio K_{abs} (a) the choice of the dipole cross section; (b) the choice of Λ_{eff} and (c) the choice of R_q.

easy to check that $f_{p\to n\pi} > f_{p\to\Lambda K}$. Moreover $\sigma_{\gamma\pi} \geq \sigma_{\gamma K}$. These two inequalities make the leading neutron cross section bigger than the leading Lambda one. The absorption correction is given by Eq. (13) and it is governed by the dipole-Lambda (or dipole-neutron) cross section, $\sigma_{d\Lambda}$. In the same way as $\sigma_{\gamma\pi} \geq \sigma_{\gamma K}$, we have $\sigma_{dn} \geq \sigma_{d\Lambda}$. These two inequalities explain why the leading Lambda is less suppressed than the leading neutron.

Finally, in Fig. 6 we show the dependence of the ratio K_{abs} on (a) the choice of the dipole cross section, and on the values of (b) Λ^2_{eff} and (c) R_q. We can see that the predictions are almost insensitive to the model assumed for σ_{dp} and to the value of R_q, which is expected since these quantities are present on the numerator and on the denominator of Eq. (14). In contrast, K_{abs} is strongly dependent on Λ^2_{eff}, since the latter determines the magnitude of the absorptive corrections, as already demonstrated in Fig. 2(b).

A final comment about the feasibility of Lambda detection in ep collisions is in order. This subject was discussed in detail in Refs. [3,36–38]. These studies have indicated that the main Λ decay channels which can be used for the experimental separation are the $\Lambda \to p\pi^-$ and $\Lambda \to n\pi^0$ processes. The Λ has a long lifetime and will be close to the proton beam with a small scattering angle. Therefore, in order to separate the leading Λ events, the detector should have the tagging capability in the hadron-going far forward region. For the current EIC project, which considers only one interaction region, the results presented in Ref. [3] indicated that the acceptance of the Λ decay products in the far forward system is larger and appropriate for ep collisions with smaller center-of-mass energies. This situation can be improved if a second detector, with a better tagging capability at forward rapidities, is installed in the near future [3].

IV. SUMMARY

In this paper we have investigated leading Λ production in future ep colliders using the color dipole formalism and estimated, for the first time, the impact of the absorptive corrections in the associated spectrum. Our analysis has been motivated by the perspective of using this process to measure the kaon structure function and improve our understanding of the partonic structure of this meson. We have presented predictions for the kinematical ranges that will be probed by the future EIC and LHeC. Our results indicate that leading Λ spectra are not strongly energy dependent at small photon virtualities. Moreover, we have estimated the impact of the absorptive effects, demonstrated that they increase at smaller photon virtualities and that they depend on the longitudinal momentum x_L.

Our main conclusion is that a realistic measurement of the γK cross sections in future colliders and the extraction of the kaon structure function must take into account the important contribution of the absorptive effects. Future experimental data on leading Λ production in ep collisions at the EIC will be crucial to test the main assumptions of our model, as well as to improve our understanding of this important observable.

ACKNOWLEDGMENTS

This work was partially financed by the Brazilian funding agencies CNPq, CAPES, FAPESP, FAPERGS, and INCT-FNA (Process No. 464898/2014-5). K. P. K. and A. M. T. gratefully acknowledge support from the Fundação de Amparo à Pesquisa do Estado de São Paulo (FAPESP), Processes No. 2022/08347-9 and No. 2023/01182-7.

APPENDIX: MESON-BARYON CROSS SECTIONS

As it was mentioned in the main text, it is very important to have a good estimate of the dipole-Lambda cross section. We need to impose constraints on this quantity. The first one is that it should be of the same order of magnitude as that of the dipole-proton cross section, which is well known. However this may not be enough, since factors of 2 or 3 may significantly change the predictions of the absorption factor. Moreover it is crucial to make predictions for higher energies (for LHeC) and also for lower energies (JLAB). In this appendix we discuss the meson-baryon

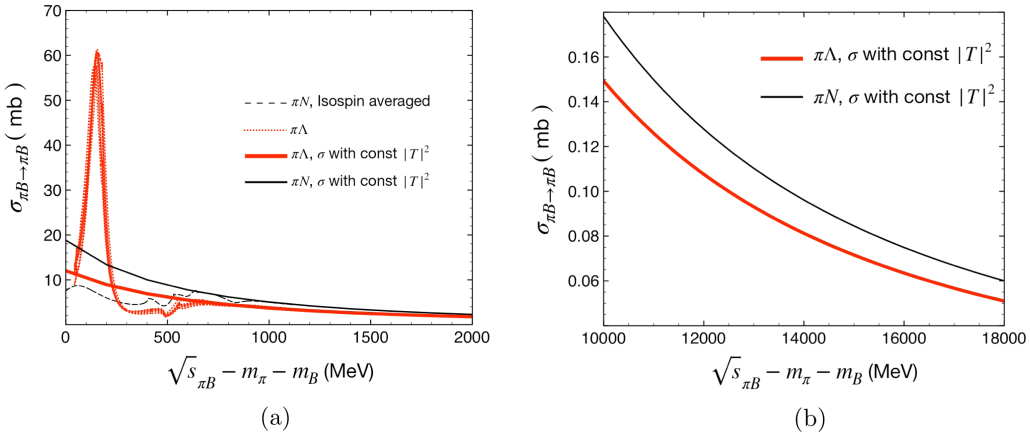

FIG. 7. π-baryon cross sections. (a) Lower energies. (b) Extrapolation to higher energies.

cross sections at lower energies. In particular we estimate the π-nucleon and π-hyperon cross sections. The comparison of these cross sections should give (or not) support to the choice of the factor r_s used in the main text.

To determine the relation between the πN and $\pi\Lambda$ cross sections we follow Refs. [31,32], which consider effective Lagrangians based on the hidden local symmetry approach [39] and treat pseudoscalar baryons and vector baryons as coupled channels. Using effective Lagrangians for the vector-pseudoscalar-pseudoscalar, vector-vector-vector, and vector-baryon-baryon vertices, t-, u-, s-channels contributions as well as contact terms were considered in Refs. [31,32] to determine the amplitudes V_{ij} describing the transitions $PB \to PB$, $VB \to VB$, and $PB \to VB$. These amplitudes are projected on the s-wave, isospin, and spins $1/2$ and $3/2$. Using the latter amplitudes, the Bethe-Salpeter equation,

$$T = V + VGT, \tag{A1}$$

is then solved in a coupled-channel approach, with V and G being matrices in the coupled channel space. The elements of V are the amplitudes V_{ij} describing the transition from a channel i to a channel j formed by pseudoscalar-baryon (PB) or vector-baryon particles (VB). The G in Eq. (A1) has, as elements, the corresponding PB and VB loop functions, which are regularized with either a cutoff of $\sim$600 MeV or dimensional regularization. In particular,

$$G_k = i2M_k \int \frac{d^4q}{(2\pi)^4} \frac{1}{(p-q)^2 - M_k^2 + i\epsilon} \frac{1}{q^2 - m_k^2 + i\epsilon}, \tag{A2}$$

where p is the total four-momenta and M_k (m_k) is the baryon (meson) mass of the channel k. We refer the reader to Refs. [31,32] for the precise expressions of the elements of V.

By solving Eq. (A1), the two-body T-matrix for the system is determined and poles in the complex energy plane which can be associated with known states [like $N^*(1535)$, $N^*(1650)$, $\Lambda(1405)$] are found. The parameters of the model are constrained to reproduce the data on cross sections like $K^-p \to K^-p$, $\bar{K}^0n$, $\eta\Lambda$, $\pi^0\Lambda$, $\pi^0\Sigma^0$, $\pi^\pm\Sigma^\mp$. The CLAS data for $\gamma p \to K^+\Lambda(1405)$ are also well reproduced [40]. For strangeness -1, channels like $\bar{K}N$, $\pi\Sigma$, $\pi\Lambda$, $\eta\Sigma$, $K\Xi$, $\bar{K}^*N$, $\rho\Lambda$, $\rho\Sigma$, $\omega\Sigma$, $K^*\Xi$, $\phi\Sigma$ were considered as coupled in Ref. [32]. In this way, a transition like $\pi\Lambda \to \pi\Lambda$ can have contributions from, for example, a virtual $\pi\Sigma$ channel. For strangeness 0, channels like πN, ηN, $K\Lambda$, $K\Sigma$, ρN, ωN, ϕN, $K^*\Lambda$, $K^*\Sigma$ are treated as coupled channels when solving Eq. (A1) [31].

In Fig. 7 we show the results for the $\pi N \to \pi N$ and $\pi\Lambda \to \pi\Lambda$ cross sections. The results shown as dashed and dotted lines, in Fig. 7(a), correspond to the πN and $\pi\Lambda$ cross sections, respectively, obtained by using the amplitudes of Refs. [31,32]. The total spin is $1/2$ in both cases, while the cross sections shown for the $\pi N \to \pi N$ are isospin averaged. It is important to mention here that the $\pi\Lambda$ cross sections correspond to a set of curves since all of them lead to similar quality of fits in Ref. [32]. Though some structures are seen at energies near the threshold, which correspond to the appearance of resonances, the cross sections for excitation energies ($\sqrt{s}_{\pi B} - m_\pi - m_B$) above 1000 MeV attain a smooth dependence in both πN and $\pi\Lambda$ cases. It seems then reasonable for the purpose of an estimation of the cross section ratios at higher energies, to extrapolate the results to such energies by considering the corresponding T-matrices to remain constant beyond some point.

We show, in Fig. 7, the cross sections obtained by considering a constant amplitude multiplied to the phase space as solid lines. The former is the value of the amplitude determined at the highest energy in Refs. [31,32]. As can be seen from Fig. 7(a), such cross sections (obtained with a constant amplitude) do not describe the structures at low

energies (shown by dashed lines) but do completely agree with the results of Refs. [31,32] beyond the excitation energies of 1000 MeV.

Thus, basically the energy dependence of the πN and $\pi\Lambda$ cross sections follows the corresponding phase space. Such behavior, if extrapolated to higher energy regions [see Fig. 7(b)], can provide an estimation of the ratio between the cross sections of πN and $\pi\Lambda$, yielding $\sigma_{\pi\Lambda} \simeq 0.83\sigma_{\pi N}$ for $\sqrt{s} \simeq 11$–19 GeV.

[1] K. Kovařík, P. M. Nadolsky, and D. E. Soper, Rev. Mod. Phys. **92**, 045003 (2020).

[2] F. Gelis, E. Iancu, J. Jalilian-Marian, and R. Venugopalan, Annu. Rev. Nucl. Part. Sci. **60**, 463 (2010); H. Weigert, Prog. Part. Nucl. Phys. **55**, 461 (2005); J. Jalilian-Marian and Y. V. Kovchegov, Prog. Part. Nucl. Phys. **56**, 104 (2006).

[3] D. Boer, M. Diehl, R. Milner, R. Venugopalan, W. Vogelsang, D. Kaplan, H. Montgomery, S. Vigdor *et al.*, arXiv:1108.1713; A. Accardi, J. L. Albacete, M. Anselmino, N. Armesto, E. C. Aschenauer, A. Bacchetta, D. Boer, W. Brooks *et al.*, Eur. Phys. J. A **52**, 268 (2016); E. C. Aschenauer, S. Fazio, J. H. Lee, H. Mäntysaari, B. S. Page, B. Schenke, T. Ullrich, R. Venugopalan, and P. Zurita, Rep. Prog. Phys. **82**, 024301 (2019); R. Abdul Khalek, A. Accardi, J. Adam, D. Adamiak, W. Akers, M. Albaladejo, A. Al-bataineh, M. G. Alexeev, F. Ameli, P. Antonioli *et al.*, Nucl. Phys. **A1026**, 122447 (2022); V. D. Burkert, L. Elouadrhiri, A. Afanasev, J. Arrington, M. Contalbrigo, W. Cosyn, A. Deshpande, D. I. Glazier, X. Ji, S. Liuti *et al.*, Prog. Part. Nucl. Phys. **131**, 104032 (2023); R. Abir, I. Akushevich, T. Altinoluk, D. P. Anderle, F. P. Aslan, A. Bacchetta, B. Balantekin, J. Barata, M. Battaglieri, C. A. Bertulani *et al.*, arXiv:2305.14572.

[4] J. L. Abelleira Fernandez *et al.* (LHeC Study Group), J. Phys. G **39**, 075001 (2012); P. Agostini *et al.*, J. Phys. G **48**, 110501 (2021).

[5] A. C. Aguilar, Z. Ahmed, C. Aidala, S. Ali, V. Andrieux, J. Arrington, A. Bashir, V. Berdnikov, D. Binosi, L. Chang *et al.*, Eur. Phys. J. A **55**, 190 (2019).

[6] J. D. Sullivan, Phys. Rev. D **5**, 1732 (1972).

[7] H. Holtmann, G. Levman, N. N. Nikolaev, A. Szczurek, and J. Speth, Phys. Lett. B **338**, 363 (1994).

[8] B. Kopeliovich, B. Povh, and I. Potashnikova, Z. Phys. C **73**, 125 (1996).

[9] M. Przybycien, A. Szczurek, and G. Ingelman, Z. Phys. C **74**, 509 (1997).

[10] N. N. Nikolaev, J. Speth, and B. G. Zakharov, arXiv:hep-ph/9708290.

[11] R. J. Holt and C. D. Roberts, Rev. Mod. Phys. **82**, 2991 (2010).

[12] B. Z. Kopeliovich, I. K. Potashnikova, B. Povh, and I. Schmidt, Phys. Rev. D **85**, 114025 (2012).

[13] J. R. McKenney, N. Sato, W. Melnitchouk, and C. R. Ji, Phys. Rev. D **93**, 054011 (2016).

[14] F. Carvalho, V. P. Goncalves, D. Spiering, and F. S. Navarra, Phys. Lett. B **752**, 76 (2016).

[15] V. P. Goncalves, D. Spiering, and F. S. Navarra, Phys. Rev. D **93**, 054025 (2016).

[16] A. Kumar and T. Toll, Phys. Rev. D **105**, 114045 (2022).

[17] A. Kumar, Phys. Rev. D **107**, 034005 (2023).

[18] U. D'Alesio and H. J. Pirner, Eur. Phys. J. A **7**, 109 (2000).

[19] B. Z. Kopeliovich, H. J. Pirner, I. K. Potashnikova, K. Reygers, and I. Schmidt, Phys. Rev. D **91**, 054030 (2015).

[20] V. A. Khoze, A. D. Martin, and M. G. Ryskin, Phys. Rev. D **96**, 034018 (2017).

[21] A. B. Kaidalov, V. A. Khoze, A. D. Martin, and M. G. Ryskin, Eur. Phys. J. C **47**, 385 (2006).

[22] V. A. Khoze, A. D. Martin, and M. G. Ryskin, Eur. Phys. J. C **48**, 797 (2006).

[23] E. Levin and S. Tapia, Nucl. Phys. **A892**, 1 (2012).

[24] F. Carvalho, V. P. Gonçalves, F. S. Navarra, and D. Spiering, Phys. Rev. D **103**, 034021 (2021).

[25] E. Iancu, K. Itakura, and S. Munier, Phys. Lett. B **590**, 199 (2004).

[26] G. Soyez, Phys. Lett. B **655**, 32 (2007).

[27] K. Golec-Biernat and S. Sapeta, J. High Energy Phys. 03 (2018) 102.

[28] M. E. Bracco, F. S. Navarra, and M. Nielsen, Phys. Lett. B **454**, 346 (1999).

[29] R. J. Glauber, in *Lecture in Theoretical Physics*, edited by W. E. Brittin and L. G. Duham (Interscience, New York, 1959), Vol. 1.

[30] E. G. S. Luna, M. J. Menon, and J. Montanha, Nucl. Phys. **A745**, 104 (2004).

[31] K. P. Khemchandani, A. Martinez Torres, H. Kaneko, H. Nagahiro, and A. Hosaka, Phys. Rev. D **84**, 094018 (2011); K. P. Khemchandani, A. Martinez Torres, H. Nagahiro, and A. Hosaka, Phys. Rev. D **88**, 114016 (2013);

[32] K. P. Khemchandani, A. Martinez Torres, and J. A. Oller, Phys. Rev. C **100**, 015208 (2019).

[33] S. Gjesdal, G. Presser, P. Steen, J. Steinberger, F. Vannucci, H. Wahl, K. Kleinknecht, V. Lüth, and G. Zech, Phys. Lett. **40B**, 152 (1972).

[34] D. Bassano, C. Y. Chang, M. Goldberg, T. Kikuchi, and J. Leitner, Phys. Rev. **160**, 1239 (1967).

[35] J. Olsson *et al.* (H1 Collaboration), Proc. Sci. DIS2014 (**2014**) 156; V. Andreev *et al.* (H1 Collaboration), Eur. Phys. J. C **74**, 2915 (2014); F. D. Aaron *et al.* (H1 Collaboration), Eur. Phys. J. C **68**, 381 (2010).

[36] G. Xie, C. Han, R. Wang, and X. Chen, Chin. Phys. C **46**, 064107 (2022).

[37] A. C. Aguilar, Z. Ahmed, C. Aidala, S. Ali, V. Andrieux, J. Arrington, A. Bashir, V. Berdnikov, D. Binosi, L. Chang *et al.*, Eur. Phys. J. A **55**, 190 (2019).

[38] A. Bylinkin, C. T. Dean, S. Fegan, D. Gangadharan, K. Gates, S. J. D. Kay, I. Korover, W. B. Li, X. Li, R. Montgomery *et al.*, Nucl. Instrum. Methods Phys. Res., Sect. A **1052**, 168238 (2023).

[39] M. Bando, T. Kugo, and K. Yamawaki, Nucl. Phys. **B259**, 493 (1985).

[40] S. H. Kim, K. P. Khemchandani, A. Martinez Torres, S. i. Nam, and A. Hosaka, Phys. Rev. D **103**, 114017 (2021).